JOURNAL OF CATALYSIS 147, 163–170 (1994)

Vapour-Phase Aromatic Nitration with Dinitrogen Tetroxide over Solid Acids: Kinetics and Mechanism

A. Germain,[1] T. Akouz, and F. Figueras

Laboratoire de Chimie Organique Physique et Cinétique Chimique Appliquées, URA 418 du C.N.R.S., Ecole Nationale Supérieure de Chimie, 8 Rue de l'Ecole Normale, 34053 Montpellier Cedex 1, France

Received February 17, 1993; revised October 4, 1993

The mechanism of the vapour-phase mononitration of aromatics with dinitrogen tetroxide has been investigated over silica–alumina and the large-pore zeolite β (BEA). A Rideal–Eley rate law is observed in both cases, showing that the reaction occurs between the chemisorbed aromatic and the gaseous nitrating agent. The effects of substituents are better correlated by a relation between the activity and the ionisation potential of the aromatic than by the Hammett equation. Both results conflict with the "classical" electrophilic aromatic substitution (SEAr), but agree with the formation of an aromatic radical cation intermediate at the surface of the catalyst and its reaction with a nitrogen dioxide radical in the rate determining step. The generation of electron-acceptor sites on the catalyst surface by nitrogen dioxide radicals is suggested. Addition of water in the feed inhibits the reaction by competitive adsorption over silica–alumina, but improves the efficiency of BEA, certainly by "steam cleaning" of the surface of this hydrophobic catalyst.

INTRODUCTION

Nitration is one of the most important electrophilic aromatic substitution reactions (1) and is widely used in the preparation of chemicals. The industrial reaction is still usually achieved with the conventional sulfonitric mixture, so-called "mixed acid." However, despite the high reactivity and the low cost of the reagents, the use of sulfuric acid suffers from a number of shortcomings, for instance, corrosion and environmental problems. Its replacement by a novel technology based on solid catalysts is highly desirable.

Since the early work of Wilhelm (2), various solids have been proposed for nitration, such as "Nafion" (3), grafted or supported benzenesulfonic acids (4), supported phosphoric acid, sulfuric acid or sulfur trioxide (5), mixed metal oxides (6), silica–alumina, clays, and zeolites (7). In most cases, the gaseous nitrating agent is dinitrogen tetroxide which is dissociated to an equilibrium mixture with nitrogen dioxide. In this condition, the nitration can be represented by the equation

$$2\mathrm{ArH} + 3\mathrm{NO_2}^{\cdot} \rightarrow 2\mathrm{ArNO_2} + \mathrm{NO}^{\cdot} + \mathrm{H_2O}.$$

Taking into account that nitric oxide readily combines with oxygen forming nitrogen dioxide (8), the stoichiometry of the reaction under air is

$$2\mathrm{ArH} + 2\mathrm{NO_2}^{\cdot} + \tfrac{1}{2}\mathrm{O_2} \rightarrow 2\mathrm{ArNO_2} + \mathrm{H_2O}.$$

Despite its industrial impact, this reaction has not been the subject of mechanistic considerations, unlike the homogeneous liquid phase nitration.

In this paper, we report a kinetic study of the vapour phase nitration of aromatics by dinitrogen tetroxide, catalyzed by acid aluminosilicates, and discuss the potential mechanisms in the light of the results. For this study two different catalysts were selected, namely an amorphous silica–alumina (SA) containing 13% alumina and a crystalline large-pore zeolite β (BEA) with a three-dimensional channel system and a ratio Si/Al = 27. Fluorobenzene was chosen for the main study on account of its volatility, its low reactivity, and the presence of one substituent strongly bound to the aromatic ring.

EXPERIMENTAL

1. Catalysts

Zeolite BEA was synthesized in the presence of tetraethylammonium hydroxide (TEAOH) according to the procedure described by Wadlinger *et al.* (9). The zeolite appeared as spheroids with sizes between 0.5 and 1 μm. This solid was calcined at 723 K, then converted to the ammonium form by ion exchange in a 0.5 *M* solution of $\mathrm{NH_4NO_3}$. Calcination at 723 K gave the protonic form with a specific surface area (BET) of 675 $\mathrm{m^2\ g^{-1}}$.

A commercial silica–alumina (Ketjen) with a specific surface area of 410 $\mathrm{m^2\ g^{-1}}$ was calcined at 773 K before

---

[1] To whom correspondence should be addressed.

0021-9517/94 $6.00

use. Poisoning of this solid was carried out by exchange for 20 h at room temperature, in a 0.1 *M* solution of the selected sodium salt (1 ml per g).

Acidity measurements were carried out, as previously described (10), by stepwise thermal desorption (STD) of ammonia.

2. *Reactants*

Dinitrogen tetroxide (Air Liquide) and all organic reagents (Fluka or Aldrich) were used without further purification. The term "substrate" in this paper will signify the organic reactant.

3. *Procedure*

The reactions were performed in a fixed-bed continuous flow microreactor operating at atmospheric pressure. The catalyst (10 mg) was mixed with inactive silica (40 mg). The reactants were fed by passing the carrier gas (air) through two parallel saturators kept at constant temperatures. At the temperature of the saturator (between − 10°C and 0°C), dinitrogen tetroxide is not dissociated (<0.1%) (8). On the contrary, its dissociation into nitrogen dioxide radicals is complete at the temperature of the reaction (140°C) (8). According to these features we assumed that the partial pressure of nitrogen dioxide in the reactor was twice the partial pressure of dinitrogen tetroxide in the saturator. The reactor effluent was analysed on line by a gas chromatograph equipped with an apolar capillary column and a flame ionisation detector.

Kinetic conditions ensuring the absence of external diffusion limitation were determined by the study of the effect of variation of the space velocity on the rate of the reaction, the partial pressure of reactants being constant.

RESULTS

1. *General Features of the Reaction*

As expected (1), the vapour-phase nitration of fluorobenzene is an irreversible reaction. This was confirmed by the absence of denitration or isomerisation of *ortho*- and *para*-nitrofluorobenzene in the most drastic conditions used for the direct reaction.

a. Activity and stability. The evolution of the activity of the silica-alumina as a function of time on stream is shown in Fig. 1. A significant deactivation occurs at the beginning of the reaction. Various standard models of decay (11) were tested, but none were in agreement with all the experimental data. In fact, graphical application of the exponential deactivation law, $\mathrm{Ln}v = \mathrm{Ln}v_0 - k_d \cdot t$, where v is the rate at time t and k_d the deactivation rate constant, leads to the observation of two linear parts (Fig. 2). Thus, the catalytic activity decreases in two successive first order processes: there is an initial fast one (k_d = 84 × 10^{-6} s^{-1}) followed by a slow one (k_d = 4.5 × 10^{-6} s^{-1}). The activity of the second part is recovered by stopping the feed for 30 min, while the restoration of the initial activity is obtained by calcination at 450°C.

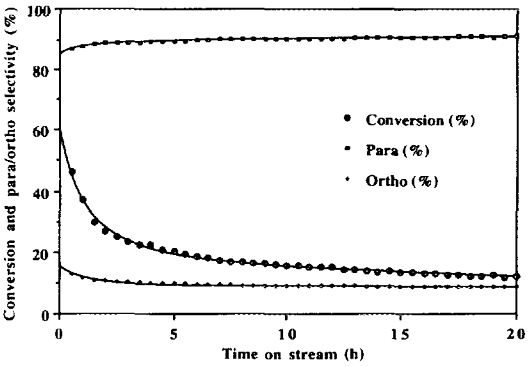

FIG. 1. Conversion and *ortho*/*para*-selectivity as a function of time on stream in the nitration of fluorobenzene over silica–alumina 13%. θ = 160°C; space velocity = 22 h^{-1}; P_{FB} = 36 Torr; $P_{N_2O_4}$ = 40 Torr.

In order to determine the role of the acidity, partial neutralisation of the acid sites of the silica–alumina was performed by the exchange of protons with sodium cations. The extent of the exchange increased with the base strength of the counter-ion ($Cl^- \ll CO_3^{2-} < PO_4^{3-}$). The acid strength distributions were determined by stepwise thermal desorption of ammonia. Comparison of the values determined for the original silica–alumina and the silica–alumina treated with sodium phosphate (Fig. 3) shows that the strongest acidities are eliminated by the exchange.

The effects of the acidity on the activity profile are presented in Fig. 2 and Table 1. The initial activity is reduced by the neutralisation, following the sequence: $SA > SA(Cl^-) \gg SA(CO_3^{2-}) > SA(PO_4^{3-})$. The initial fast deactivation rate is reduced by exchange with NaCl and suppressed when the silica–alumina is neutralised by Na_2CO_3 or Na_3PO_4.

From these results two conclusions can be drawn: one is that the activity is correlated with the acidity of the

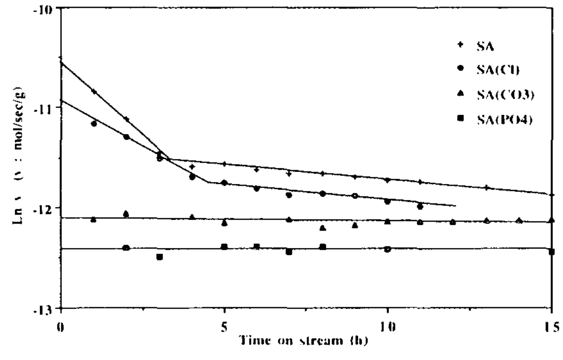

FIG. 2. Effect of sodium exchange on the activity of silica–alumina. Same conditions as Fig. 1.

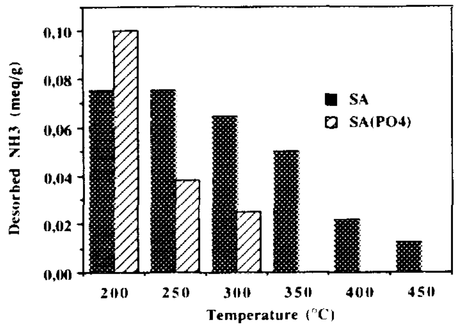

FIG. 3. Acid strength distribution determined by stepwise thermal desorption of ammonia.

catalyst and the other that the fast deactivation is connected with the strongest acid sites of silica–alumina.

b. Selectivity. Below 180°C, only the mononitrated compounds are produced. The *para*-isomer is predominant (85–94%) with a very low proportion of the *meta*-isomer (0.2–0.5%). This agrees with the results of the nitration of fluorobenzene using "mixed acid" (12).

In the course of the deactivation of silica–alumina, the *para*-selectivity increases slightly from 86 to 91% (Fig. 1). Furthermore, the initial *para*-proportion also increases with the neutralisation of the strong acidity by sodium salts (Table 1). This signifies that the most active (or acid) centres are the least favourable for the predominant *para*-nitration, which is in agreement with the classical activity–selectivity relationship (13).

2. *Kinetics of the Reaction*

The kinetic experiments were performed after the first deactivation step, taking the mode of evolution of the activity into account.

A preliminary study was performed to determine the conditions (temperature and space velocity) required to ensure the absence of external diffusion limitation and a low conversion rate (<5%). Using these conditions, it was accepted that the products had no effect on the rate of the reaction.

The possible influence of internal diffusion effects was estimated using the criterion of Weisz (14): $\varphi = (dN/dt)(1/c_0)(R^2/D_{\mathrm{eff}})$, in which dN/dt is the reaction rate (mol s^{-1} cm^{-3}), c_0 the concentration of the reactant (mol cm^{-3}), R the particle radius (cm) and D_{eff} the effective diffusivity (cm^2 s^{-1}). At an average pressure of reactant of 20 Torr, the reaction rate is about 5×10^{-6} mol s^{-1} g^{-1}, with zeolite BEA ($\varnothing < 1$ μm). Assuming, in these conditions, that the diffusion coefficient of the reactant is of the order of 10^{-6} cm^2 s^{-1}, which appears reasonable for wide-pore zeolites and amorphous silica–alumina, the value of φ is about 10^{-2}, which ensures that mass transport does not limit the rate.

a. Influence of the partial pressure of the reactants. The dependence of the specific rate of nitration as a function of the partial pressure of nitrating agent is reported in Fig. 4. For both catalysts a linear relationship is observed, indicating a first order reaction.

The rate is not proportional to the partial pressure of the aromatic reactant but tends to be constant for high pressures as shown in Fig. 5. We believe that this reduction of the order when the pressure increases is not due to liquid condensation, as proposed by Giannetto *et al.* (15). The highest pressure of fluorobenzene used (6×10^{-2} bar) is very low compared to the vapour pressure at the temperature of the reaction (≈4 bar). The most probable explanation is the saturation of the active sites of the catalyst, according to the Langmuir isotherm. Plotting the reciprocal of the rate versus the reciprocal of the pressure gives a straight line (Fig. 6).

For our experiments we can assume that the reaction takes place between the chemisorbed aromatic and the nitrating agent in the gas phase, in accordance with the Rideal–Eley mechanism. The rate constants k and the adsorption coefficients of fluorobenzene λ_{FB}, are deduced from the rate law: $v = k \cdot P_{\mathrm{N_2O_4}} \cdot P_{\mathrm{FB}}/(1 + \lambda_{\mathrm{FB}} \cdot P_{\mathrm{FB}})$.

TABLE 1

Characteristics and Catalytic Properties of Na-Exchanged Silica–Alumina

Catalyst	SA	SA(Cl)	SA(CO$_3$)	SA(PO$_4$)
Na content (%)	<0.01	0.15	≈4	≈4
Acidity (meq g^{-1})	0.34			0.16
Initial activity (10^{-6} mol s^{-1} g^{-1})	27	18	5.6	4.0
Initial deactivation (10^{-6} s^{-1})	84	54	0.9	≈0
para-Selectivity (%):				
Initial	86	88	88.5	90
At 10 h	91	91	90	90.5

Note. (Same conditions as Figure 2.)

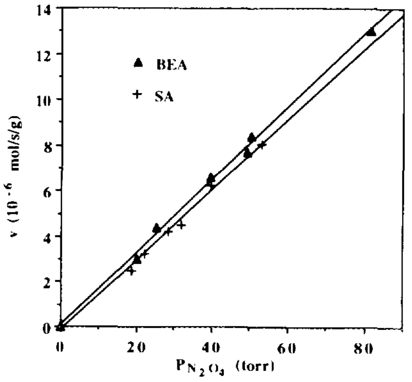

FIG. 4. Rate of nitration of fluorobenzene as a function of partial pressure of N_2O_4. $\theta = 140$°C; $P_{\mathrm{FB}} = 15.9$ Torr; space velocity = 72 h^{-1}.

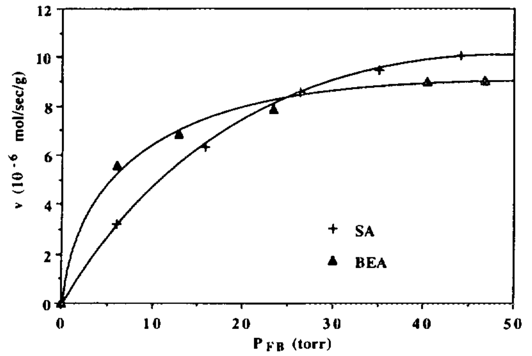

FIG. 5. Rate of nitration of fluorobenzene as a function of partial pressure of fluorobenzene. θ = 140°C; $P_{N_2O_4}$ = 40 Torr; space velocity = 72 h^{-1}.

TABLE 2

Rate Constants (*k*) and Adsorption Coefficients of Fluorobenzene (λ_{FB}) at 140°C, and Activation Energies in the Nitration of Fluorobenzene by N_2O_4

Catalyst	*k* (mol s^{-1} g^{-1} $Torr^{-1}$)	λ_{FB} ($Torr^{-1}$)	$E^{\neq}$ (kcal mol^{-1}) Total	*para*	*ortho*
SA	3.9 10^{-7}	0.048	14.6	12.8	16.2
BEA	2.3 10^{-7}	0.240	11.8	11.3	13.1

The values for each catalyst are given in Table 2. It must be pointed out that fluorobenzene is more strongly adsorbed on zeolite BEA than on silica–alumina.

b. Influence of added water. Since water is a product of the reaction, we decided to determine its influence on the kinetics. The addition of water in the feed produces two opposite effects on the activity, depending on the nature of the catalyst (see Fig. 7):

— Over silica–alumina, water inhibits the nitration by competitive adsorption. Application of the rate law, $v = k \cdot P_{N_2O_4} \cdot P_{FB}/(1 + \lambda_{FB} \cdot P_{FB} + \lambda_{H_2O} \cdot P_{H_2O})$ in the reciprocal form (Fig. 8) allows the determination of the adsorption coefficient of water: $\lambda_{H_2O} = 0.60\,Torr^{-1}$. Water is much more strongly adsorbed on silica–alumina than fluorobenzene, which is in agreement with the expected hydrophilicity of this catalyst. Therefore, at high conversion, it is likely that part of the deactivation of this catalyst is due to the adsorption of produced water.

— Over zeolite BEA, water exhibits an opposite effect. On addition of 3 Torr of water, the activity is increased by 20%, then is stabilized for higher pressures. The absence of inhibition over zeolite BEA can be justified by the low hydrophilicity of this catalyst and its high capacity for adsorption of aromatics. Thus, water does not compete with fluorobenzene. On the other hand, the explanation of the increase in activity is not so evident. Considering that the kinetic experiments are carried out over partially deactivated catalysts, a regeneration of the active surface by water can be suspected. This could be due to a "steam distillation" of some adsorbed heavy products such as, for example, dinitrocompounds. Such a hypothesis has already been proposed in order to explain the stabilisation of the activity in the conversion of ethylene and ethanol over zeolite H-ZSM-5 in the presence of water (16, 17).

Whatever the catalyst, the addition of water and the variation of the partial pressures of the reactants have no influence on the *para*/*ortho*-selectivity.

c. Influence of the temperature. This study was performed under partial pressure ensuring a zero-order with respect to fluorobenzene. Below 200°C, the reaction obeys the Arrhenius law. The activation energies, given in Table 2, are slightly lower than the ones reported for the nitration of fluorobenzene in sulfonitric solution (14–18 kcal mol^{-1}) (12). The lower values obtained with zeolite BEA certainly reflect the stronger acidity of the active sites of this catalyst.

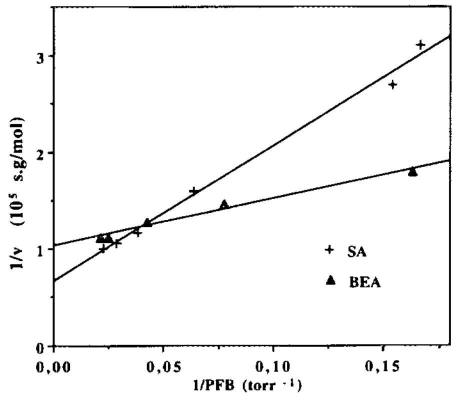

FIG. 6. Reciprocal of the rate of nitration of fluorobenzene as a function of reciprocal of the partial pressure of fluorobenzene. Same conditions as Fig. 5.

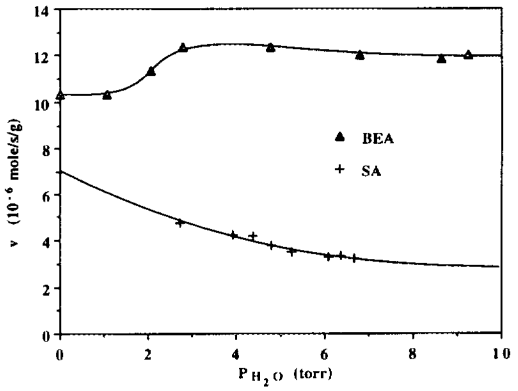

FIG. 7. Influence of added water on the rate of nitration of fluorobenzene. θ = 140°C; P_{FB} = 27 Torr; $P_{N_2O_4}$ = 31 Torr; space velocity = 122 h^{-1}.

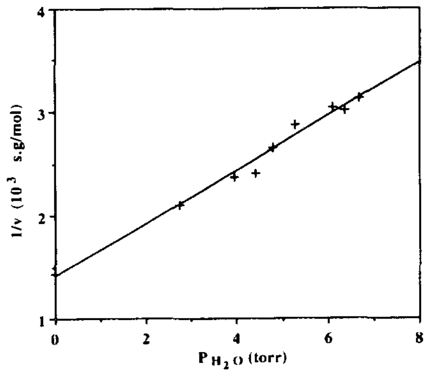

FIG. 8. Reciprocal of the rate of nitration of fluorobenzene over silica-alumina as a function of partial pressure of added water. Same conditions as Fig. 7.

Above 200°C, the variation of the rate as a function of the temperature is reduced. This could be due to several reasons: One is that the chemical process becomes so fast that it is limited by the diffusion of the reactants; a second is that the order with respect to the adsorbed substrate is no longer zero, so that the energy of activation is reduced by the enthalpy of adsorption, and a third is that the catalyst is deactivated at high temperature by the formation of secondary products.

The temperature has also an influence on the proportion of the isomers, as shown Fig. 9. The *para*-selectivity is seen to decrease with increasing temperature. This is expressed in the highest activation energy being that for the nitration in the *ortho*-position (Table 2). It should be noted that this effect is more important with silica-alumina than with zeolite BEA and that the *para*-selectivity is always higher with this latter catalyst. However, from a comparison of various zeolites, to be published in a subsequent paper, no relationship between the selectivity of position and the pore size of the catalyst could be deduced.

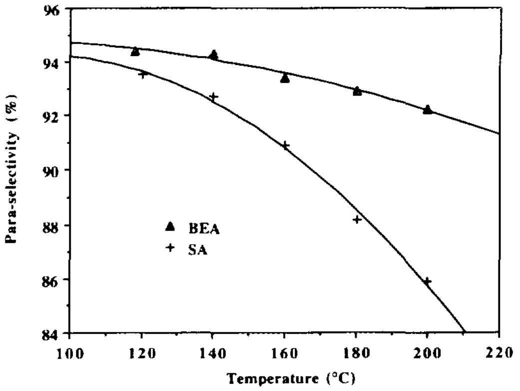

FIG. 9. *para*-Selectivity (%) in the nitration of fluorobenzene as a function of the temperature. P_{FB} = 35.6 Torr; $P_{N_2O_4}$ = 40 Torr; space velocity = 163 h^{-1}.

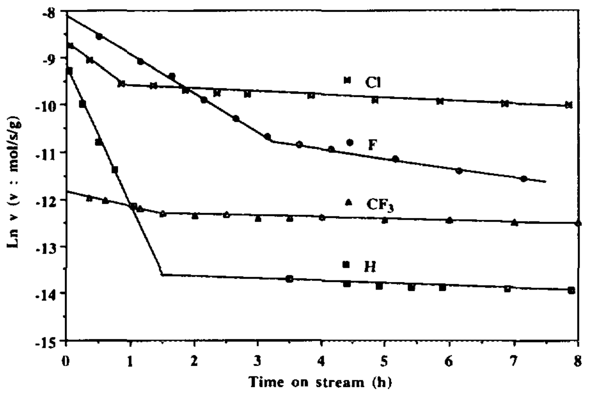

FIG. 10. Activity of zeolite BEA as a function of time on stream in the nitration of various aromatics.

3. *Effect of Substituents*

The study of the effect of substituents on the reactivity of the benzene ring can give information on the mechanism of the reaction. For example, the nitration in sulfuric acid (12), with most of the "classical" electrophilic aromatic substitution reactions (SEAr), obeys the Hammett equation (18) using Brown's σ^+ constants (19): $\log(k/k_0) = \rho \cdot \sigma^+$. The application of this equation has already been extended to the heterogeneous catalysis of various reactions (20–22).

In order to eliminate the effect of the differences in adsorption of the substrates, the reactions were performed under saturation of the active surface, i.e., under conditions of zero-order with respect to the aromatic. From technical considerations, the study was restricted to the most volatile compounds: benzene, toluene, fluorobenzene, chlorobenzene, and trifluoromethyl benzene (α, α, α-trifluorotoluene). The evolution of the activity (Lnv) of zeolite BEA as a function of time on stream is shown in Fig. 10 for the different aromatics. As previously observed, the deactivation occurs in two steps, but with large variations in the rates depending on the nature of the aromatic. Toluene is excluded from the results because of the complete deactivation of the catalyst in less than 30

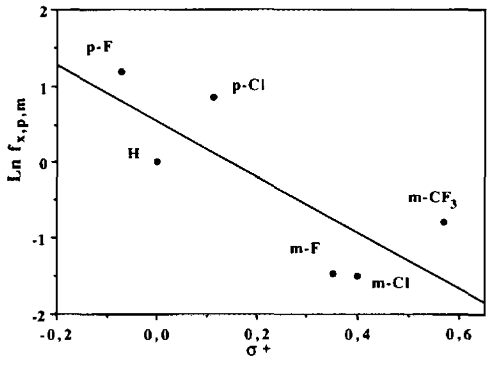

FIG. 11. Plot of the Hammett equation.

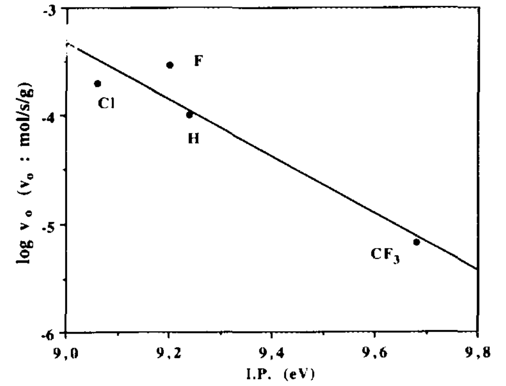

FIG. 12. Initial activities (log v_0) as a function of the ionization potential of the aromatics.

min. This fast deactivation is accompanied by the formation of numerous by-products. Taking into account the differences in the rates of deactivation, the effects of the substituents were studied by comparison of the initial activities determined by extrapolation.

The validity of the Hammett equation is tested in Fig. 11. The logarithms of the partial rate factors f (with $f_{p,mX} = v_{p,mX}/v_H$) are plotted against the substituent constant σ^+ (18, 19) for the different aromatics. A very poor correlation is obtained (correlation coefficient $R = 0.80$). Attempts to apply the modifications proposed by Yukawa and Tsuno (23): $\log f = \rho[\sigma + r(\sigma^+ - \sigma)]$, where r is a measure of the contribution of the resonance effect on the reactivity, failed as well. Likewise, the activity is not satisfactorily correlated with the proton affinity of the substrates, although the protonation represents a prototype of electrophilic attack on the aromatic nucleus (24, 25).

A better agreement is obtained between the logarithm of the initial rates and the ionization potential of the aromatics (26, 27), as shown in Fig. 12 (correlation coefficient $R = 0.93$). This result is an argument in favour of the involvement of the radical cation of the aromatic in the rate-determining step of the reaction.

DISCUSSION

According to current knowledge, the aromatic nitration by nitrogen tetroxide in the vapour phase can proceed by three different mechanisms: these are the free-radical reaction by $NO_2^{\cdot}$, the classical electrophilic attack by NO_2^+ and the one-electron transfer through the formation of an aromatic radical cation.

The free-radical mechanism, which occurs at high temperature or under irradiation, gives close to statistical product distributions. Thus, radical nitration of fluorobenzene gives about 35% of the *meta*-isomer (28), which is completely different from the present results (*meta* < 0.5%). Therefore, such a mechanism is ruled out for the heterogeneous acid-catalysed nitration.

The electrophilic mechanism requires the acid activation of the nitrating reagent in order to form the nitronium ion (1). In the subsequent step, this cation reacts with the free aromatic substrate. In opposition, an interaction between the acid catalyst (liquid, as well as solid) and the aromatic, such as ring protonation or donor–acceptor complexation, suppresses the possibility of an electrophilic attack. According to these considerations, our kinetic results are not in agreement with the electrophilic substitution mechanism. In fact, they show that the gaseous nitrating agent reacts with the chemisorbed aromatic substrate. The poor correlation for the Hammett equation (Fig. 11) is an additional argument against such an ionic mechanism.

The best correlation between the initial rates and the ionization potentials of the aromatics (Fig. 12), as we have already pointed out, is in fact in favour of the formation of the radical-cation of the aromatic. Furthermore, such an intermediate can easily explain the large formation of secondary products and the very fast deactivation in the nitration of toluene. Effectively, removal of an electron from toluene drastically enhances its C–H acidity (29). Then, the formation of the benzyl radical leads to side-chain nitration or oxidation and radical coupling (30). Such secondary reactions produce high boiling compounds which are poisons for the catalyst; see Scheme 1.

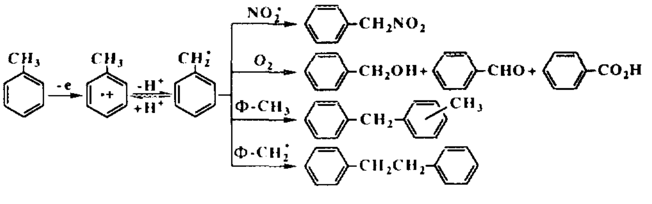

SCHEME 1

The possibility of a one-electron transfer in aromatic nitration, first suggested by Kenner (31) and Weiss (32), was developed by Perrin in 1977 (33). According to this author, an electron transfer occurs from the aromatic to the nitronium ion, followed by the collapse of the radical-pair to the σ-complex intermediate.

$$ArH + NO_2^+ \rightleftharpoons ArH^{\cdot +}, NO_2^{\cdot} \rightleftharpoons ArHNO_2^+ .$$

Since then, the electron transfer abilities of the nitronium ion have been the subject of significant discussions (34–36).

The formation of the aromatic radical cation in the present heterogeneous catalysis is not dependent on the nitronium ion. According to the kinetic results, the activation of the substrate is due to its chemisorption on the catalyst. Thus, we propose that the reaction is initiated by the formation of the aromatic radical cation on the surface and that the attack of this adsorbed species by a free radical $NO_2^{\cdot}$ constitutes the rate-determining step.

The formation of organic radical cations on silica–alumina and zeolites has been known for a long time (37, 38), but the nature of the electron acceptor has always been the subject of controversy. Metal impurities such as Fe^{3+} (39), or defects formed during calcination (40, 41), have been proposed as electron acceptor sites; however, the mechanism mostly considered is an electron transfer to a Lewis acid site generated during high temperature pretreatment of the catalyst (38, 42). The presence of oxygen could activate the electron transfer (43–46). However, in the present case, the effect of water, which increases the activity of zeolite BEA, is not really in accordance with the participation of Lewis acid in the nitration. Moreover, the reduction of the activity by sodium cation exchange is rather indicative of the action of Brønsted acids. In order to reconcile the electron acceptor property with the protonic acidity, we propose the formation of radicals at the surface of the catalyst by abstraction of hydrogen atoms from the hydroxyl sites by nitrogen dioxide radicals. This reaction also allows the regeneration of the catalytic sites. This is shown in the first equation of the following scheme. The second step is an electron transfer from the aromatic to the radical at the surface, leading to the adsorbed radical cation. The rate-determining step is the subsequent addition of a nitrogen dioxide radical to this species giving the σ-complex. The deprotonation of this complex constitutes the final fast step which produces the nitrocompound and regenerates the acid catalyst. Then, a new catalytic cycle can occur.

$$\text{Catal–OH} + NO_2^{\cdot} \rightleftharpoons \text{Catal–O}^{\cdot} + HNO_2$$

$$\text{Catal–O}^{\cdot} + ArH \rightleftharpoons \text{Catal–O}^{-}, ArH^{\cdot +}$$

$$\text{Catal–O}^{-}, ArH^{\cdot +} + NO_2^{\cdot} \rightarrow \text{Catal–O}^{-}, ArHNO_2^{+}$$

$$\text{Catal–O}^{-}, ArHNO_2^{+} \rightarrow \text{Catal–OH} + ArNO_2$$

$$ArH + N_2O_4 \rightarrow ArNO_2 + HNO_2$$

According to this scheme the reaction produces nitrous acid, which was not observed. In fact, in the gas phase, this acid is dehydrated (47, 48) and the so-formed dinitrogen trioxide is oxidized in air.

$$2HNO_2 \xrightarrow{-H_2O} N_2O_3 \rightleftharpoons NO^{\cdot} + NO_2^{\cdot} \xrightarrow{+\frac{1}{2}O_2} 2NO_2^{\cdot} \rightleftharpoons N_2O_4$$

Finally, we reach the stoichiometry of the overall reaction already given in the Introduction.

$$2ArH + 2NO_2^{\cdot} + \tfrac{1}{2}O_2 \rightarrow 2ArNO_2 + H_2O$$

The influence of the acidity of the catalyst on the activity is justified by the stabilisation of the radical cation at the surface.

The loss of activity is assigned to the formation and the adsorption of traces of heavy secondary products such as dinitrofluorobenzenes. Coking (i.e., polycondensation of aromatic nuclei) seems improbable at the temperature of the reaction. Confirmation of this assumption will be presented in a subsequent paper.

CONCLUSION

Unlike the usual sulfonitric procedure, the heterogeneous vapour-phase nitration of aromatics does not conform to the expected "classical" ionic mechanism. The kinetic results are in better agreement with a one-electron transfer process leading to an aromatic radical cation at the surface of the catalyst. This is followed by the combination of this cation with a free nitrogen dioxide radical. Such a mechanism is similar to the one proposed some years ago by Perrin (33) and by Achord and Hussey (49) for the electro-assisted nitration of naphthalene by dinitrogen tetroxide in aprotic solvents. In our case, the presence of gaseous nitrogen dioxide is invoked for the generation of electron-acceptor sites on the surface of the catalyst by hydrogen abstraction from the Brønsted acid sites. Zeolite BEA proved to be an effective catalyst. The addition of water in the feed, which inhibits the reaction over the hydrophilic silica–alumina, improves the efficiency of the zeolitic catalyst. The comparison of the activity and stability of various zeolites, in preparative conditions, will be the topic of a further publication.

REFERENCES

1. For a review see: (a) Schofield, K., "Aromatic Nitration." Cambridge Univ. Press, Cambridge, 1980; (b) Olah, G. A., Malhotra, R., and Narang, S. C., "Nitration Methods and Mechanisms. Organic Nitro Chemistry Series." Verlag Chemie, Weinheim, 1989.
2. Wilhelm, R. H., U.S. Patent 2,109,873 (1936).
3. Lawrence, F. R., U.S. Patent 4,234,470 (1980).
4. (a) Suzuki, S., Tohmori, K., and Ono, Y., *Chem. Lett.* 747 (1986); (b) Suzuki, E., Tohmori, K., and Ono, Y., *Chem. Lett.* 2273 (1987).
5. (a) Schubert, H., and Wunder, F., U.S. Patent 4,112,006 (1978); (b) Schumacher, I., and Wang, K. B., U.S. Patent 4,347,389 (1982) and Eur. Patent 78,247 (1985); (c) Sumitomo Chemical Co., Japan Patent 58,180,459 (1983).
6. Sato, I., and Nakamura, S., Japan Patent 58,162,557 (1982), and Eur. Patent 92,372 (1985).
7. (a) Shimada, K., Nishikawa, T., Harada, T., and Nagahama, S., U.S. Patent 3,966,830 (1976); (b) Bakke, J. M., and Liaskar, J., U.K. Patent 2,000,141 (1978); (c) Owsley, D. C., and Bloomfield, J. J., U.S. Patent 4,107,220 (1978); (d) Sumitomo Chemical Co., Japan Patent 58,157,748 (1983); (e) Japan Synthetic Rubber Co., Japan Patent 59,216,851 (1983).
8. Cotton, F. A., and Wilkinson, G., *in* "Advanced Inorganic Chemistry. A Comprehensive Text," 4th ed., p. 423. Wiley, New York, 1980.

9. Wadlinger, R. L., Kerr, G. T., and Rosinski, E. J., U. S. Patent 3,308,069 (1967).
10. Chauvin, B., Boulet, M., Massiani, P., Fajula, F., Figueras, F., and Des Courrières, T., *J. Catal.* **126,** 532 (1990).
11. Szépe, S., and Levenspiel, O., *Chem. React. Eng.*, 265 (1971).
12. Combes, R. G., Crout, D. H. G., Hoggett, J. G., Moodie, R. B., Schofield, K., *J. Chem. Soc.* (*B*), 347 (1970).
13. Pross, A., *Adv. Phys. Org. Chem.* **14,** 69 (1972).
14. Weisz, P. B., *Chem. Eng. Progr. Symp. Ser.* **55,** 29 (1957).
15. Giannetto, G., Perot, G., Guisnet, M., *Acta Phys. Chem.* **31,** 467 (1985).
16. Védrine, J. C., Dejaifve, P., Naccache, C., Derouane, E. G., *Stud. Surf. Sci. Catal.* **7A,** 724 (1981).
17. Oudejans, J. C., van den Oosterkamp, P. F., and van Bekkum, H., *Appl. Catal.* **3,** 109 (1982).
18. Johnson, C. D., "The Hammett Equation." Cambridge Univ. Press, London, 1973.
19. Stock, L. M., and Brown, H. C., *Adv. Phys. Org. Chem.* **1,** 35 (1963).
20. Kraus, M., and Bazant, V., *in* "Catalysis," Vol. 2, p. 1073. Elsevier, New York, 1973.
21. Chiche, B., Finiels, A., Gauthier, C., and Geneste, P., *Appl. Catal.* **30,** 365 (1987).
22. Pardillos, J., Coq, B., Brunel, D., Massiani, P., de Menorval, L. C., and Figueras, F., *J. Amer. Chem. Soc.* **112,** 1313 (1990).
23. Yukawa, Y., and Tsuno, Y., Bull. *Chem. Soc. Jpn* **39,** 971 (1959).
24. Lau, Y. K. and Kebarle, P., *J. Amer. Chem. Soc.* **98,** 7452 (1976).
25. McKelvey, J. M., Alexandratos, S., Streitweiser, A., Abboud, J.-L. M., and Hehre, W. J., *J. Amer. Chem. Soc.* **98,** 244 (1976).
26. Streitweiser, A., *Progr. Phys. Org. Chem.* **1,** 1 (1963).
27. Rosenstock, H. M., Drakl, K., Steiner, B. W., and Herron, J. T., *J. Phys. Chem. Ref. Data, Suppl.* **6,** 1 (1977).
28. Olah, G. A., and Overchuck, N. A., *Canad. J. Chem.* **43,** 3279 (1965).
29. Bordwell, F. G., and Cheng, J. P., *J. Amer. Chem. Soc.* **111,** 1792 (1989).
30. Suzuki, H., *Synthesis,* 217 (1977).
31. Kenner, J., *Nature* **156,** 369 (1945).
32. Weiss, J., *Trans. Faraday Soc.* **42,** 116 (1946).
33. Perrin, C. L., *J. Amer. Chem. Soc.* **99,** 5516 (1977).
34. Eberson, L., and Radner, F., *Acc. Chem. Res.* **20,** 53 (1987).
35. Morkovnik, A. S., *Russ. Chem. Rev. Engl. Trans.* **57,** 144 (1988).
36. Kochi, J. K., *Angew. Chem. Int. Ed. Engl.* **27,** 1227 (1988).
37. Rooney, J. J., and Pink, R. C., *Trans. Faraday Soc.* **58,** 1632 (1963).
38. Stamires, D. N., and Turkevich, J., *J. Amer. Chem. Soc.* **86,** 749 (1964).
39. Zholobenko, V. L., Kustov, L. M., and Kazansky, V. B., *Kinet. Katal.* **30,** 901 (1989).
40. Shih, S., *J. Catal.* **79,** 390 (1983).
41. Kucherov, A. V., Slinkin, A. A., Kondratyev, D. A., Bondarenko, T. N., Rubinstein, A. M., and Minachev, K. M., *J. Mol. Catal.* **37,** 107 (1986).
42. Bandiera, J., Ben Taarit, Y., and Naccache, C., *Bull. Soc. Chim. Fr.*, 3419 (1969).
43. Kodratoff, J., Naccache, C., and Imelik, B., *J. Chim. Phys.* **65,** 562 (1968).
44. Ben Taarit, Y., Naccache, C., and Imelik, B., *J. Chim. Phys.* **67,** 389 (1970).
45. Dollish, F. R., and Hall, W. K., *J. Phys. Chem.* **71,** 1005 (1967).
46. Chen, F. R., and Fripiat, J. J., *J. Phys. Chem.* **96,** 819 (1992).
47. Ashmore, P. G., and Tyler, B. J., *J. Chem. Soc.*, 1017 (1961).
48. Asquith, P. L., and Tyler, B. J., *J. Chem. Soc. Chem. Commun.*, 744 (1970).
49. Achord, J. M., and Hussey, C. L., *J. Electrochem. Soc.* **128,** 2556 (1981).